



ELSEVIER

Biochimica et Biophysica Acta 1507 (2001) 100–114

BIOCHIMICA ET BIOPHYSICA ACTA

BBA

www.bba-direct.com

Review

Electron transfer in photosystem I

Klaus Brettel *, Winfried Leibl

Section de Bioénergétique and CNRS URA 2096, Département de Biologie Cellulaire et Moléculaire, CEA Saclay, 91191 Gif-sur-Yvette Cedex, France

Received 11 December 2000; received in revised form 31 May 2001; accepted 18 June 2001

Abstract

This mini-review focuses on recent experimental results and questions, which came up since the last more comprehensive reviews on the subject. We include a brief discussion of the different techniques used for time-resolved studies of electron transfer in photosystem I (PS I) and relate the kinetic results to new structural data of the PS I reaction centre. © 2001 Elsevier Science B.V. All rights reserved.

Keywords: Photosystem I; Electron transfer; Phylloquinone; Iron–sulfur cluster

1. Introduction

After the purple bacterial reaction centre [13], photosystem I (PS I) is the second photosynthetic reaction centre for which a highly resolved X-ray structure has been obtained [17,30]. An important difference from the purple bacterial reaction centre is that PS I contains a chain of four low potential ($E_m < -500$ mV versus NHE) secondary electron acceptors, the phylloquinone A_1 and three [4Fe–4S] clusters named F_X , F_A and F_B (see [7,21] for more comprehensive reviews on PS I). Relating structure and function of PS I may hence provide an original and essential contribution to the understanding of the principles of solar energy conversion developed by nature and – more generally – of electron transfer processes in proteins (note that photosynthetic elec-

tron transfer can be triggered by a short flash of light, allowing kinetic studies with high time-resolution).

The physiological function of PS I is to catalyse light-driven transfer of electrons from reduced plastocyanin or cytochrome c_6 located in the lumen to ferredoxin in the stroma. As oxidation and reduction of the redox partners occur on opposite sides of the membrane, PS I has to provide an efficient electron transfer pathway across the membrane. This electron transfer pathway is realised by a chain of cofactors bound to the reaction centre protein at different levels within the membrane. From a functional point of view, light absorption leads to formation of the excited state of the primary donor, P700, followed by electron transfer to a primary acceptor, A_0 . The electron is then further transferred along a series of secondary electron acceptors, A_1 , F_X , F_A , and F_B , thereby crossing the membrane.

Fig. 1 presents the arrangement of the cofactors susceptible to be involved in electron transfer in PS I. P700 is a chlorophyll (Chl) dimer composed of a Chl a' (eC-A1) and Chl a (eC-B1). Two nearly sym-

Abbreviations: Chl, chlorophyll; DMF, dimethylformamide; EPR, electron paramagnetic resonance; NHE, normal hydrogen electrode; PS I, photosystem I; SCE, standard calomel electrode

* Corresponding author. Fax: +33-1-6908-8717.

E-mail address: brettel@dsvidf.cea.fr (K. Brettel).

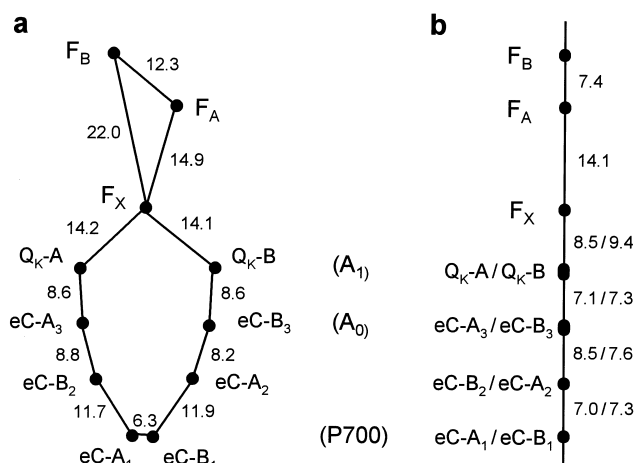


Fig. 1. Schematic representation of the arrangement of the electron transfer cofactors in PS I based on the 2.5-Å structure ([30,17] and P. Jordan, P. Fromme, N. Krauss, personal communication). Centre-to-centre distances (a) and their projection onto the normal to the membrane (b) are given in Å. eC-A_{*i*} and eC-B_{*i*} (*i* = 1, 2, 3) denote Chl *a* (or – for eC-A₁ – Chl *a*′) molecules bound to subunits PsaA and PsaB, respectively. Q_K-A and Q_K-B denote phylloquinone molecules bound to PsaA and PsaB, respectively. The other symbols are explained in the text. Distances were measured between the Mg²⁺ ions of chlorophylls, the midpoints of the oxygen atoms of phylloquinones, and the centroids of iron–sulphur clusters. The presentation is adapted from [32].

metric branches of cofactors are present between P700 and F_X, each composed of two chlorophylls (eC-B2/eC-A2 and eC-A3/eC-B3) and a phylloquinone (Q_K-A/Q_K-B). Whether the two branches are used with similar probability or whether one of them is clearly dominating is presently debated (see Section 3.1). The first spectroscopically resolved electron acceptor, A₀, is assumed to be represented by chlorophyll eC-A3 and/or eC-B3. Chlorophyll eC-B2 and/or eC-A2 is presumably in some way involved in electron transfer from excited P700 to A₀ (see Section 3.3). These six chlorophylls, the two phylloquinones and the [4Fe–4S] cluster F_X are bound by two large (~83 kDa), highly homologous subunits, PsaA and PsaB, while the two terminal electron acceptors, the [4Fe–4S] clusters F_A and F_B, are bound by the small (~9 kDa), stromal subunit PsaC.

A simplified scheme of the kinetics and energetics of electron transfer in PS I is presented in Fig. 2. The primary electron transfer steps (from excited P700 via A₀ to A₁) are ultrafast processes (picosecond time scale) with a considerable driving force. Elec-

tron transfer from A₁[–] via F_X to F_A and F_B has presumably a lower driving force (note that the reduction potential of A₁[–] is not well established; see Section 3.2). The reoxidation of A₁[–] occurs in tens to hundreds of nanoseconds; the further transfer to F_A and F_B is only poorly characterised (see Section 2.2).

Several techniques have been applied to study kinetics of electron transfer in photosystem I. The most abundant kinetic information was obtained by absorption change measurements. These measurements are based on the characteristic difference spectra of reduced and oxidised forms of the cofactors in the visible, UV, and near-IR spectral region. The accessible time window is very large, ranging from the sub-ps to seconds time scale. Limitations of this technique are mainly due to overlapping or similar absorption features of different cofactors, which are the same chemical species. This makes measurements of electron transfer from the P700 to the primary acceptors (all partners are chlorophyll molecules) or between the iron–sulphur centres difficult. Another difficulty is connected with the strong background absorption due to the presence of a large number of antenna chlorophylls in normal PS I preparations. Absorption changes due to singlet and triplet excited states of antenna pigments can be superimposed to the absorption changes due to electron transfer. A novel spectrophotometric technique [1] permits detection of small flash-induced absorption changes down to a nanosecond time scale even in intact cells [29].

Transient electron paramagnetic resonance (EPR) spectroscopy has been applied to follow the spin-polarised radical pair P700⁺A₁[–] on a time scale from 10 ns to several microseconds (at room temperature), and to characterise magnetic interactions in this pair (see review by van der Est [68] in this issue). An advantage of this technique is its selectivity for paramagnetic species, so that antenna pigments do normally not interfere.

In oriented samples transmembrane electron transfer can be detected by measurements of the kinetic changes in the membrane potential (photovoltage). Unlike spectroscopic techniques, these measurements cannot provide direct information on the chemical nature and interactions of the molecules involved in the electron transfer reaction. However, besides the kinetic information, photovoltage measurements pro-

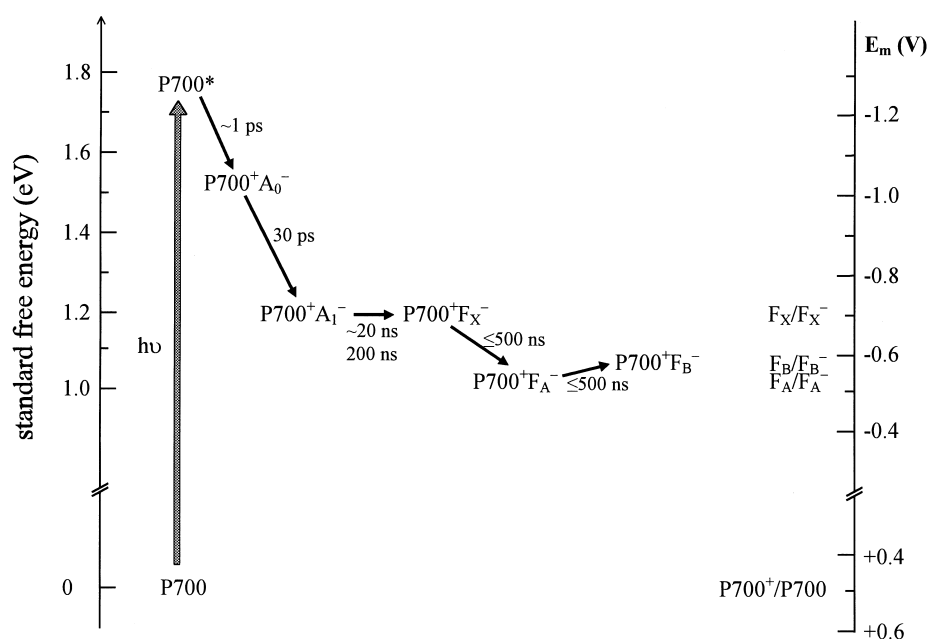


Fig. 2. Approximate standard free energy levels and kinetics of charge separation in PS I. The standard free energy of the dark state (P700) was arbitrarily set to zero. Reduction midpoint potentials (versus NHE) obtained by redox titrations of intact PS I are indicated on the right-hand scale. If interactions between the cofactors are negligible, the standard reaction free energy ΔG^0 (per molecule) for the formation of a pair P^+A^- from PA is related to the reduction potentials by

$$\Delta G^0(\text{PA} \rightarrow \text{P}^+\text{A}^-) = q_e[E_m(\text{P}^+/\text{P}) - E_m(\text{A}/\text{A}^-)] \quad (1)$$

where q_e is the elementary charge. See text for further details, references and discussion.

vide the electrogenicity of individual reaction steps. The electrogenicity is proportional to the dielectrically weighted transmembrane distances over which electron transfer occurs, and therefore contains structural information about the relative transmembrane distances between cofactors (when a homogeneous dielectric environment is assumed). The transmembrane organisation (see Fig. 1b) of the electron transfer pathway in PS I makes this system particularly suited for this kind of measurements. Advantages of photovoltage measurements are their inherent selectivity for electrogenic events, a high time resolution and an excellent signal-to-noise ratio. On the other hand, it should be kept in mind that electrogenic relaxations might contribute to a measured potential change. Another difficulty of the photovoltage measurements is related to the fact that different techniques are necessary for measurements on a sub- μs time scale [66] and for slower measurements (see, e.g., [65]), and that the time windows of both techniques do hardly overlap.

2. Recent data on electron transfer in PS I

2.1. Primary electron transfer (from excited P700 via A_0 to A_1)

The intrinsic time constant of the first step of charge separation in PS I is difficult to determine, because the intact PS I RC contains about 100 antenna chlorophylls that absorb photons and transfer excitation energy amongst them and to P700 in a few picoseconds. Hence, the apparent rate of charge separation (in the order of 30 ps) is slower than the intrinsic rate that would be observed in the absence of antenna chlorophylls upon excitation of P700. In addition, estimations of the intrinsic rate of charge separation from measured rates are dependent on the kinetic limitations, i.e., whether the excited state decay kinetics is trap limited or transfer limited. The model of excitation trapping in PS I is, however, still debated (see review by Gobets and van Grondelle [19] in this issue). Recent simulations of time-re-

solved absorption and fluorescence data yielded an intrinsic time constant of 770 fs [2] or 620 fs [18] or 500 fs [12] for electron transfer from excited P700 to the first electron acceptor, which is faster than previous estimates of 1–3 ps (reviewed in [7]). In contrast, from an analysis of the calculated difference between kinetics at 690 nm in open centres (P700 reduced prior to excitation) and in closed centres (P700 oxidised prior to excitation), a time constant of 9–10 ps was attributed to electron transfer from excited P700 to A_0 in PS I from *Synechocystis* sp. PCC 6803 [56]. A critical condition for the validity of this analysis is that the energy transfer processes in open and closed centres are identical, so that the difference signal represents exclusively electron transfer processes. As the absorbance changes due to excitation and energy transfer between antenna pigments were more than 10 times bigger than those attributed to electron transfer [56], the result of the subtraction might be affected already by subtle differences in energy transfer between open and closed centres. In [56], the overall excitation energy trapping times at P700 (~ 24 ps) were found to be very nearly the same in open and closed centres, justifying the subtraction procedure. Another study, however, reported a 10% increase in excitation energy lifetime upon closing the PS I reaction centre of *Synechococcus elongatus* [12]. Summarising, the intrinsic rate of primary charge separation in PS I appears to be still uncertain.

To our knowledge, there is no direct kinetic evidence that a chlorophyll-like species other than P700 and A_0 functions as a real intermediate in charge separation, although the arrangement of the cofactors suggests such a role for the chlorophyll eC-B2 and/or eC-A2 (see Section 3.3).

The time constant of electron transfer from A_0^- to A_1 had been estimated previously from kinetic absorption spectroscopy monitoring the reoxidation of A_0^- to $\tau \approx 30$ ps (reviewed in [7]), which is close to the value of about 50 ps deduced from photovoltage measurements [25]. A recent paper [11] reported direct monitoring of the reduction of the phyloquinone A_1 by ultrafast spectroscopy in the near-UV absorption band of A_1^- around 380 nm. The flash-induced absorption transients averaged over 380 to 390 nm increased with a time constant of 30 ps. The spectrum of the absorption changes reached at 150

ps after excitation (measured between 380 and 480 nm) resembles the spectrum at 2 ns after excitation, obtained by conventional kinetic absorption spectroscopy and attributed to the state $P700^+A_1^-$. It was concluded that electron transfer from A_0^- to A_1 occurs directly and completely with $\tau \approx 30$ ps.

In another ultrafast study [46], a 28 ps phase observed in the blue spectral region was interpreted as due to overall excited state decay by electron transfer forming the state $P700^+A_1^-$. A striking result of this study is that the spectrum of the absorbance changes remaining after completion of the 28 ps phase shows a bleaching in the near-UV (measured down to 380 nm). This feature is in contrast to the ultrafast study [11] mentioned above and to several studies in nanosecond and microsecond time scales [7–10,29,39,45,63] where formation of the state $P700^+A_1^-$ was characterised by a broad absorption increase around 380 nm, largely due to the absorption of the phylosemiquinone anion A_1^- . As the near-UV bleaching reported in [46] challenges the previous absorption studies on electron transfer involving A_1 , it would be important to check whether there is an important spectral evolution up to the nanosecond range under the experimental conditions used in [46]. Such a study might also give hints whether species not involved in electron transfer (e.g., singlet excited state of uncoupled antenna chlorophylls) contribute to the spectra on the picosecond time scale.

The same study [46] presents an ($A_1^- - A_1$) difference spectrum in the 380 to 490 nm range obtained by subtracting a ($P700^+ - P700$) difference spectrum (measured on a 100-ms time scale using a conventional transient absorption set-up) from the spectrum of the absorbance changes remaining after completion of the 28 ps phase. The resulting spectrum shows a pronounced absorption increase around 430 nm and a bleaching around 400 nm, and has generally the shape of an inverted ($P700^+ - P700$) spectrum. While a bleaching around 400 nm is in contrast to previous work (see above), the ($A_1^- - A_1$) difference spectrum around 430 nm was previously not well established [6,7,10]. Because of the dominating bleaching due to oxidation of P700 around 430 nm, ($A_1^- - A_1$) spectra obtained by subtraction of the ($P700^+ - P700$) spectrum from spectra for the formation of the state $P700^+A_1^-$ are very sensitive to proper normalisation. On the other hand, electron trans-

fer from A_1^- to F_X ($t_{1/2} = 10\text{--}200$ ns; see Section 2.2) should be accompanied by a pronounced bleaching around 430 nm if the ($A_1^- - A_1$) spectrum were to show a pronounced absorption increase (F_X bleaches around 430 nm upon reduction [21]). However, only a weak bleaching with kinetics in the 10 to 200 ns range has been observed around 430 nm [6,8,29,63]. Hence, unless the unusual ($A_1^- - A_1$) spectrum in [46] should be due to a poor normalisation of the two experimental spectra subtracted, there would have to be considerable spectral evolution between about 100 ps and a few nanoseconds after excitation, a time range that has not yet been directly examined in PS I.

2.2. Secondary electron transfer (from A_1^- to the iron-sulphur clusters F_X , F_A and F_B)

Pathway, kinetics and energetics of secondary electron transfer in PS I are still a matter of debate. While the reoxidation of A_1^- could be studied by time-resolved absorption and EPR spectroscopy as well as photovoltage, data on the subsequent electron transfer between F_X , F_A , and F_B are scarce and mostly based on more indirect approaches.

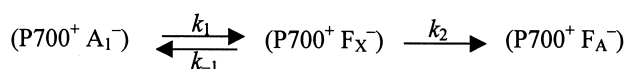
For PS I complexes isolated from spinach, flash induced absorbance changes in the near-UV, attributed to the reoxidation of A_1^- , showed biphasic kinetics with $t_{1/2} \approx 20$ ns and 150 ns (amplitude ratio about 2:1) [63]; transient EPR of a spin-polarised signal attributed to the state ($P700^+A_1^-$) resolved the 150 ns phase, but not the 20 ns phase, presumably because of insufficient time-resolution [5,67]. As a possible explanation for the biphasic reoxidation of A_1^- , it was suggested [63] that the free energies of the states $P700^+A_1^-$ and $P700^+F_X^-$ are close to each other, i.e., the forward and backward electron transfer rates k_1 and k_{-1} (see Scheme 1) are similar. In this model, establishment of a quasi-equilibrium between $P700^+A_1^-$ and $P700^+F_X^-$ gives rise to a fast phase of A_1^- reoxidation, and depopulation of this quasi-equilibrium by electron transfer from F_X^- to the next ac-

ceptor (now known to be F_A ; see below) gives rise to the slower phase.

For PS I isolated from cyanobacteria, only a single phase of A_1^- reoxidation ($t_{1/2} \approx 200$ ns) had been observed [6,63]. More recently, however, with an improved time resolution of 2 ns, a phase with $t_{1/2} = 7$ ns (representing about one third of the total decay of A_1^-) was discovered in PS I from the cyanobacterium *Synechocystis* sp. PCC6803 [8]. In terms of the $A_1^- - F_X$ equilibrium model outlined above, these data imply that for PS I from *Synechocystis*, the state $P700^+F_X^-$ would be about 20 meV higher in free energy than the state $P700^+A_1^-$, whereas in PS I from spinach, $P700^+F_X^-$ would be about 40 meV below $P700^+A_1^-$ [8]. As the PS I complexes from spinach used in these studies were isolated by a rather harsh treatment, it was speculated that the pronounced 20 ns phase in these samples might result from a modification of the PS I complex during isolation [63].

Using a novel spectrophotometric technique, Joliot and Joliot [29] managed to follow the reoxidation of A_1^- in whole cells of a *Chlorella sorokiniana* mutant lacking most of photosystem II and of the peripheral antennae. They observed two phases of about equal amplitude with halftimes of about 18 and 160 ns, respectively, which is close to the kinetics observed in PS I isolated from spinach and does not support the idea of a preparation artefact being responsible for the biphasic kinetics in spinach PS I.

In order to verify the $A_1^- - F_X$ equilibrium model, Joliot and Joliot [29] studied the effect of the membrane potential (varied by the presence or absence of uncoupler) on the reoxidation kinetics of A_1^- . The rationale was that a change in the membrane potential should affect the equilibrium between $P700^+A_1^-$ and $P700^+F_X^-$ and hence – in the framework of the $A_1^- - F_X$ equilibrium model – the relative amplitudes of the two phases of A_1^- reoxidation. The absence of any significant effect of the membrane potential on the observed kinetics of A_1^- led Joliot and Joliot to consider the $A_1^- - F_X$ equilibrium model as unlikely and to assume $k_1 \gg k_{-1}$, i.e., that $P700^+A_1^-$ is well above $P700^+F_X^-$ in free energy [29]. As alternative explanations for the biphasic reoxidation of A_1^- , they suggested that either PS I is present under two conformational states which differ by the reoxidation rate of A_1^- , or that two phyloquinones (most likely



Scheme 1.

Q_K -A and Q_K -B, see Fig. 1) are involved in electron transfer to F_X with different rates (see Section 3.1).

The slower one of the two phases of A_1^- reoxidation has been studied as a function of temperature in PS I from *S. elongatus* [57]. Between 300 and 200 K, the rate slowed down according to an activation energy of 220 meV; below 200 K, forward electron transfer from A_1^- via F_X to F_A and F_B was partially replaced by charge recombination in the pairs $P700^+A_1^-$ and $P700^+F_X^-$, and a kinetic heterogeneity of PS I became obvious below 150 K: in about 45% of the PS I complexes, forward electron transfer was blocked at the level of A_1 , in about 20% at the level of F_X , and in only about 35% reduction of F_A or F_B was possible. Possible origins of this behaviour, including the idea that conformational substates are frozen below the liquid-to-glass transition of the medium (at around 180 K in the presence of 65% glycerol) were discussed extensively [7,57].

A_1^- reoxidation in membrane fragments from *Chlamydomonas reinhardtii* as monitored by pulsed EPR was recently reported to occur with a time constant of 422 ns in a frozen suspension at 260 K (the absence of a faster phase may be due to an insufficient time resolution of the set-up) [15]. The A_1^- reoxidation was slowed down about two-fold in a mutant (PsaA: D576L) where an aspartate residue adjacent to one of the cysteine ligands of F_X was replaced by leucine, but was restored to the wild-type rate in second site suppressor mutants [15].

An interesting case are the *menA* and *menB* mutants of *Synechocystis* sp. PCC 6803 that cannot synthesise phyloquinone, but recruit a foreign quinone Q, most likely plastoquinone-9, into the A_1 site [28,60,72]. PS I complexes isolated from these mutants showed efficient forward electron transfer to F_A/F_B . The reoxidation of Q^- was biphasic with lifetimes of about 15 μ s and 250 μ s (minor phase) [60]. Based on an analysis of the electron transfer kinetics and on in vitro reduction potentials of quinones, it was concluded that electron transfer from Q^- to F_X is thermodynamically unfavourable in this mutant, but that overall transfer from Q^- to F_A/F_B is exergonic [60].

With respect to electron transfer between the iron-sulphur clusters F_X , F_A , and F_B , it has long been debated which of the two high electron densities in the PsaC subunit observed in the X-ray diffraction of

PS I crystals corresponds to F_A and which to F_B . Recent kinetic and spectroscopic data from different labs converge to the conclusion that the cluster located closer to F_X is F_A , and that the distal cluster is F_B [14,16,20,35,42,64,69], in line with a conclusion from the 2.5 Å crystal structure [17,30]. The electron transfer pathway should hence be $F_X \rightarrow F_A \rightarrow F_B$. Concerning the kinetics of these two electron transfer steps (see [7] for a review of data up to 1996), it became clear from studies on ferredoxin reduction by PS I, involving F_B [14,16,42,69] and occurring to a large extent in about 500 ns [16,38,61,62] that neither electron transfer from F_X^- to F_A , nor from F_A^- to F_B can be slower than about 500 ns. In the framework of the A_1-F_X equilibrium model (which is contested; see above), the intrinsic rate k_2 of electron transfer from F_X^- to F_A can be estimated from the measured biphasic reoxidation kinetics of A_1^- (see above), yielding $k_2 \approx (80 \text{ ns})^{-1}$ for PS I from *Synechococcus* and $k_2 \approx (170 \text{ ns})^{-1}$ for PS I from spinach [8]. By contrast, an intrinsic rate faster than $(25 \text{ ns})^{-1}$ for electron transfer from F_X^- to F_A was suggested in [29], based on the observation that the amplitude of a 25 ns phase of absorption changes attributed to a change of the membrane potential (electrochromic bandshift) was larger than expected for electron transfer from A_1^- to F_X .

In principle, time resolved photovoltage measurements (see Introduction) should be able to monitor all transmembrane electron transfer steps, including that from F_X to F_A . Experiments performed with a time resolution of 5–7 ns on PS I membranes from *Synechocystis* sp. PCC 6803 could be simulated by two phases: a fast instrument limited rise (attributed to the formation of the state $P700^+A_1^-$ [25]), and a slower monoexponential rise with $t_{1/2} \approx 150$ ns (attributed to overall electron transfer from A_1^- via F_X to F_A and possibly to F_B ¹) [14,37]. Removal of F_A and F_B by urea treatment decreased the relative amplitude of the latter phase more than two-fold, but

¹ A 7 ns phase as observed in transient absorption measurements of A_1^- reoxidation in PS I from *Synechocystis* (see above) was not detected in these photovoltage measurements. This could be due to the fact that the expected electrogenicity for the establishment of the equilibrium (7 ns phase) is weak compared to the electrogenicity of the 150 ns phase, which is due to overall electron transfer from A_1^- to F_A or F_B .

did not significantly alter its kinetics. It was concluded that the overall electron transfer from A_1^- to F_A or F_B is limited by the step from A_1^- to F_X , and that the intrinsic rate of electron transfer from F_X^- to F_A must be faster than $(50 \text{ ns})^{-1}$ [14,37]. A difficulty in these measurements was, that the directly measured signal is a convolution of the photovoltage kinetics generated by PS I with the ionic relaxation of the medium around the membrane fragments which had a characteristic time of only about 50 ns. Hence, to obtain the kinetics cited above, a convolution procedure had to be applied, which relies on the assumption that the ionic relaxation is homogeneous. In an alternative approach, 66% (v/v) glycerol was added which slowed the ionic relaxation down to about 10 μs so that it should have only a minor effect on photovoltage kinetics in the sub-microsecond range. Surprisingly, the second phase of the photovoltage rise was found to be slower ($t_{1/2} \approx 350 \text{ ns}$) than in the absence of glycerol ($t_{1/2} \approx 150 \text{ ns}$), although the reoxidation of A_1^- as monitored by transient absorption was not affected by glycerol [37]. Unless there is a technical problem with the measuring cell in the presence of glycerol, this result appears to indicate that electron transfer beyond F_X , which makes the main contribution to the electrogenicity signal, is slowed down by glycerol [37]. It is of note that the amplitude of the 150 ns phase of the photovoltage rise was only about 35–40% of the total amplitude, whereas the transmembrane distance between A_1 and F_A is about 50% of the distance between P700 and F_A (see Fig. 1b). This deviation may be due to the fact that the 7 ns phase of A_1 reoxidation was not resolved in the photovoltage measurements and/or to a higher effective dielectric constant of the environment of the electron transfer path from A_1 to F_A compared to that of the path from P700 to A_1 (note that the photovoltage amplitudes due to a charge displacement are inversely related to the dielectric constant).

With respect to electron transfer between F_A and F_B , it is of note that thermodynamically slightly favourable ($-\Delta G^\circ \approx 0\text{--}80 \text{ meV}$) transfer between the two [4Fe–4S] clusters of ferredoxins similar in structure to PsaC was found by NMR to occur in about 300 ns [34]. Hence, a time constant $\leq 500 \text{ ns}$ for electron transfer from F_A^- to F_B (as concluded from the reduction kinetics of ferredoxin; see above) seems

reasonable, provided that the reduction potential of F_A is lower or close to that of F_B , at least when ferredoxin is bound. For references and a discussion on the energetics of electron transfer between the three iron–sulphur clusters of PS I, see [7].

2.3. Charge recombination reactions

Charge recombination between $P700^+$ and the reduced form of any one of the electron acceptors can be observed when forward electron transfer to the subsequent acceptor is blocked, e.g., by prereduction or extraction of the latter (see [7] for a review of data up to 1996). Typical recombination times are some tens of nanoseconds for $P700^+A_0^-$, 10–250 μs for $P700^+A_1^-$, about 1 ms for $P700^+F_X^-$, and some tens of milliseconds for $P700^+F_A^-$ and $P700^+F_B^-$. Recombination kinetics can be affected by the reduction state of the electron acceptors not directly involved in the recombination. Thus, $P700^+A_1^-$ recombination was found to be accelerated to $t_{1/2} = 250 \text{ ns}$ when all three iron–sulphur clusters were reduced; this acceleration was attributed to an up-shift of the free energy of $P700^+A_1^-$ due to the electrostatic interaction between A_1^- and F_X^- , F_A^- , and F_B^- that favours a fast recombination of $P700^+A_1^-$ via thermally activated repopulation of the primary pair $P700^+A_0^-$ [50].

New data became available for the charge recombination reactions involving the terminal acceptors F_A and F_B . In intact PS I from *S. elongatus*, recombination between $P700^+$ and a single electron equilibrated between F_A and F_B (the equilibrium ratio of F_A^- and F_B^- is a matter of debate [7]) occurs with $t_{1/2} = 80 \text{ ms}$ at room temperature; it has an activation energy of $(220 \pm 10) \text{ meV}$ (measured between 275 and 306 K) which is consistent with a recombination pathway via thermally activated repopulation of the pair $P700^+A_1^-$ [31]. With two electrons on the F_A – F_B complex, the recombination was accelerated to $t_{1/2} \approx 10 \text{ ms}$ (at room temperature). A redox titration of the recombination kinetics yielded midpoint potentials of $(-440 \pm 10) \text{ mV}$ and $(-465 \pm 10) \text{ mV}$ for the first and second reduction of the F_A – F_B complex, respectively [31]. For unknown reasons, these potentials are considerably higher than those established previously by titrations with detection of the reduction state of the iron–sulphur clusters by low-temperature EPR (approximately -540 and -590 mV , re-

spectively; reviewed in [7]). A difference of about 50 mV between these two potentials would be consistent with the observed ratio of about eight between the recombination rates (see above), provided that both recombinations proceed by thermally activated repopulation of the same state (presumably $P700^+A_1^-$; see above).

The recombination between $P700^+$ and F_A^- after destruction of F_B by treatment of cyanobacterial PS I with $HgCl_2$ was recently studied by two groups. The reported recombination rates are $(90 \text{ ms})^{-1}$ for a PS I preparation from *Synechocystis* sp. PCC 6803 [14] and $(40.7 \text{ ms})^{-1}$ for a PS I preparation from *Synechococcus* sp. PCC 6301 [64].

3. Some controversial points

3.1. Are both electron transfer branches active?

As outlined in Section 2.2, Joliot and Joliot [29] suggested that electron transfer from excited $P700$ to F_X proceeds with similar probabilities along the two branches shown in Fig. 1, but that the last steps (Q_K-A^- to F_X and Q_K-B^- to F_X) have different rates. This model provides a simple explanation for the observed bi-phasic reoxidation ($t_{1/2} \approx 10\text{--}20 \text{ ns}$ and 200 ns) of the reduced secondary acceptor A_1 . The authors considered the previously suggested A_1-F_X equilibrium model (assuming similar free energy levels for the states $P700^+A_1^-$ and $P700^+F_X^-$ in a single active branch; see Section 2.2) as unlikely as they could not observe a significant change of the reoxidation kinetics of A_1^- upon collapse of the membrane potential [29]. Taking into account the different levels of A_1 and F_X within the membrane (see Fig. 1), it was estimated [29] that the collapse of the membrane potential should have increased the driving force of electron transfer from A_1^- to F_X by about 13 meV, and hence the equilibrium constant between the states $P700^+A_1^-$ and $P700^+F_X^-$ by a factor of 1.7. In the framework of the A_1-F_X equilibrium model, this effect should have increased the amplitude ratio of the fast and slow phase of A_1^- reoxidation by a similar factor, which should have been easily detectable. We would like to point out, however, that also in the two-branch model the kinetics of A_1^- reoxidation should be affected by the

membrane potential. For a 13 meV increase in driving force from the phyloquinones to F_X , and assuming that the reorganisation energy is large compared to the driving force, Marcus theory [43,44] predicts an acceleration by a factor of 1.3 for both phases of A_1^- reoxidation which was not reported by Joliot and Joliot [29]. Hence we feel that the lack of a significant membrane potential effect does not strongly favour the two-branch model over the A_1-F_X equilibrium model. Nevertheless, we find the two-branch model very interesting as it may account for some hitherto unexplained features of PS I. In the following, we discuss some observations and reflections, which are relevant in this context.

1. In a PS I core preparation devoid of the terminal electron acceptors F_X , F_A , and F_B , charge recombination between $P700^+$ and A_1^- was biphasic with halftimes of about $10 \mu\text{s}$ and $110 \mu\text{s}$ [9]. A straightforward explanation would be that both branches are used and that the recombination rates of Q_K-A^- and Q_K-B^- with $P700^+$ are different. As the absorption difference spectra of the two phases of forward electron transfer from A_1^- are significantly different between 450 and 480 nm [8,29,63], one would expect that the two recombination phases show a similar difference. However, at room temperature, such a difference was not observed [9]. This spectral analysis does hence not support the idea that the biphasic forward electron transfer and the biphasic recombination are in the same way related to the use of the two electron transfer branches. This is only a weak argument against the two-branch model, however, as the signal to noise ratio of the $110 \mu\text{s}$ recombination phase was rather poor. Interestingly, at cryogenic temperature (10 K) where the recombination between A_1^- and $P700^+$ was found to be biphasic as well (halftimes of $15 \mu\text{s}$ and $150 \mu\text{s}$), the spectra of the two phases were different [9]. Their difference correlates with the difference between the spectra of the two phases of forward electron transfer in a way that would be consistent with the view that the fast phase of forward electron transfer and the slow phase of recombination arise from one branch, and the slow forward and the fast recombination phases from the other branch.

2. Studies of secondary electron transfer by transient EPR spectroscopy at a time resolution of about 50 ns [5,67] could resolve only the slower one ($t_{1/2} \approx 150$ ns) of the two phases of A_1^- reoxidation observed by optical spectroscopy. The spin-polarised EPR spectrum detected at the beginning of the 150 ns phase was similar (although not identical) to the spectrum observed in a PS I core preparation devoid of F_X , F_A , and F_B [67], and was attributed to the spin-correlated, weakly coupled radical pair $P700^+A_1^-$ created by fast forward electron transfer from a singlet precursor [5,67]. Within the framework of the A_1-F_X equilibrium model, the slower phase of the reoxidation of A_1^- would be preceded by forth and back electron transfer between A_1 and F_X (see Section 3.2). The latter process is expected to diminish the spin polarisation of the excess electron on the acceptor side because F_X^- has a very fast spin relaxation rate [55]. Although we are not aware of any simulation of this scenario, it seems likely, that the transient residence of the excess electron on F_X would strongly modify the EPR spectrum of the pair $P700^+A_1^-$, in contrast to the observed similarity with the $P700^+A_1^-$ spectrum in PS I devoid of F_X , F_A , and F_B . This problem is overcome in the two-branch model, because both A_1^- reoxidation phases are due to forward electron transfer from the initially created pairs $P700^+Q_K-A^-$ and $P700^+Q_K-B^-$.
3. A single active branch was strongly favoured by reports that one out of the two phylloquinones present in intact PS I could be extracted with hexane, and that PS I retaining only one phylloquinone was fully active in forward electron transfer [4,41]. If both branches were active with similar yields in untreated PS I, removal of one phylloquinone should block forward electron transfer at the level of A_0^- and give rise to charge recombination in the primary pair $P700^+A_0^-$ in about half of the centres, in contrast to observation [4]. It is of note, however, that in a more recent study, PS I extracted with hexane according to the same protocol retained approximately two phylloquinones per P700 [59], questioning the above evidence for a single active branch.
4. EPR studies have established that a phylloquinone anion radical can be trapped (in addition to reduced F_A , F_B , and F_X) by illuminating PS I at 200–230 K under reducing conditions ([24,70], and references cited in [7]). According to a recent spin-quantification, not more than one phylloquinone radical could be accumulated in that way [40,70]; it was concluded that only one of the two phylloquinones is redox active [70]. In previous work, however, a second phylloquinone radical could be trapped under harsher conditions than those necessary to trap the first one [24]. The latter observation may be explained in the framework of the two-branch model by assuming that the two phylloquinone anion radicals recombine with $P700^+$ at rather different rates (see also (1)); as trapping of a reduced acceptor requires rereduction of $P700^+$ by an external reductant prior to charge recombination, the phylloquinone with the faster recombination rate would be more difficult to be trapped in the reduced state.
5. The A_1-F_X equilibrium model was based, among others, on the observation that the slower phase ($t_{1/2} \approx 150$ ns) of forward electron transfer from A_1^- in spinach PS I was replaced by a 250 μ s recombination with $P700^+$ upon prereduction of F_A and F_B , while the fast phase ($t_{1/2} \approx 25$ ns) of forward electron transfer was conserved [63]. This behaviour is expected if the 150 ns phase reflects electron transfer from the equilibrium between A_1^- and F_X to F_A/F_B . To explain the same behaviour in the framework of the two-branch model, one would have to assume that prereduction of F_A and F_B blocks electron transfer to F_X from one of the phylloquinones, but not from the other one. A possible mechanism would be the Coulomb interaction between the transferred electrons and F_A^-/F_B^- that tends to decrease the driving force of electron transfer from the phylloquinones to F_X . Due to the asymmetric positions of F_A and F_B (see Fig. 1), this effect is most likely more pronounced for the phylloquinone designated Q_K-A than for Q_K-B . In addition, due to differences in the surroundings of the two phylloquinones, the driving forces may be different already under normal conditions (F_A and F_B oxidised), so that the Coulomb interaction with F_A^-/F_B^- might render electron transfer from the phylloquinones to F_X uphill in one branch and leave it still downhill in the other branch.

6. Within the framework of the A_1 - F_X equilibrium model, variations of the relative amplitudes of the two phases of A_1^- reoxidation between different PS I preparations could be explained by slight variations of the free energy difference between the states $P700^+A_1^-$ and $P700^+F_X^-$. If instead the two phases were due to the two electron transfer branches, amplitude variations should be due to variations in the relative yield of charge separation in the two branches.

Concluding this discussion, none of the arguments against the two-branch model appears to be ‘water-proof’. The same is true for the arguments against the A_1 - F_X equilibrium model, except point (2), where we couldn’t find a reasonable explanation of the experimental results assuming a single active branch with an equilibrium constant close to 1 (free energy difference $\Delta G^0 \approx 0$) between the states $P700^+A_1^-$ and $P700^+F_X^-$. If future work will prove that both branches are active, this would not exclude, however, that $\Delta G^0 \approx 0$ holds for electron transfer from one of the two phylloquinones to F_X (see also (5) above and Section 3.2). An interesting question is, of course, how an asymmetric P700 (eC- A_1 is Chl a' and is involved in three hydrogen bonds, whereas eC- B_1 is Chl a without hydrogen bonds [17,30]) can transfer electrons to both branches with approximately equal yields.

3.2. The reduction potential of the phylloquinone A_1

Since the discovery of phylloquinone as secondary electron acceptor A_1 , it has been recognised that its one-electron reduction potential should be at least as low as about -700 mV versus normal hydrogen electrode (NHE) in order to allow for efficient forward electron transfer to the terminal acceptors F_A and F_B ([7] and references therein). Two important points are still subject to controversial discussions:

- The reduction potential of A_1 relative to that of F_X , or more precisely, the free energy of the state $P700^+A_1^-$ relative to that of the state $P700^+F_X^-$ (see Eq. 1 in the legend of Fig. 2).
- The reason(s) why phylloquinone in PS I has a much lower reduction potential than the structurally similar menaquinone-9 as secondary electron

acceptor Q_A in the bacterial reaction centre from *Rhodospseudomonas viridis* ($E_m \approx -150$ mV [52]).

Different approaches have been used to estimate the reduction potential of A_1 or the free energy of the state $P700^+A_1^-$:

1. Interpreting the two phases of A_1^- reoxidation in the framework of the A_1 - F_X equilibrium model (see Section 2.2), it was estimated that the state $P700^+A_1^-$ is about 40 meV above $P700^+F_X^-$ in the PS I- β preparation from spinach [63,8], and about 20 meV below $P700^+F_X^-$ in PS I from *Synechocystis* sp. PCC 6803 [8]. Obviously, these estimations are not valid if it will be confirmed that the two kinetic phases are due to the two electron transfer branches (see Section 3.1).
2. From a study of the efficiency of forward electron transfer to F_A/F_B after reconstitution of diethyl-ether extracted PS I with quinones with different in vitro reduction potentials, the potential of native phylloquinone in the A_1 site was estimated to be 50–80 mV more negative than that of F_X [26]. As pointed out previously [7], the kinetic modelling of the data was based on a very slow rate of electron transfer from F_X^- to F_A/F_B (4.6×10^3 s $^{-1}$) which is inconsistent with data on intact PS I (see Section 2.2).
3. Assuming that charge recombination of the pair $P700^+(F_A F_B)^-$ ($t_{1/2} \approx 50$ ms at room temperature) proceeds via thermal repopulation of the pair $P700^+A_1^-$ and direct charge recombination in the latter pair with $t_{1/2} \approx 150$ μ s, a free energy difference of 150 mV between $P700^+A_1^-$ and $P700^+(F_A F_B)^-$ is obtained from a simple equilibrium consideration [7]. Unfortunately, the free energy difference between $P700^+F_X^-$ and $P700^+(F_A F_B)^-$ is not well established. A value of 150–190 meV can be estimated from redox titrations of the iron–sulphur clusters in intact PS I (see [7] for references). This would imply that $P700^+F_X^-$ lies slightly above $P700^+A_1^-$ in free energy, but the free energy of $P700^+F_X^-$ may be overestimated because F_A and F_B were pre-reduced in the redox titration of F_X . A lower free energy of $P700^+F_X^-$ (about 100 meV above $P700^+F_A^-$) was estimated from a comparison of the recombination time constants for $P700^+F_X^-$ in PS I devoid

of F_A and F_B ($\tau \approx 0.85$ ms) and $P700^+F_A^-$ in PS I devoid of F_B ($\tau \approx 40.7$ ms) [64]. An uncertainty in this estimate is that the free energy levels and the recombination rates in these modified PS I complexes may be different from those in intact PS I (see also [60]). The same objection can be raised against an estimation of the free energy change for electron transfer from A_1^- to F_X (-28 meV) based on an analysis [7] of kinetic and spectroscopic data in PS I devoid of F_A and F_B . As a more general problem we would like to mention that these approaches probe the energetics on a time scale that is much slower than forward electron transfer. Energy minimising conformational changes of the protein in response to changes of the charges on the cofactors are expected to occur on multiple time scales. Hence, the free energy levels of the different charge separated states during forward electron transfer may deviate significantly from those estimated from slow recombination reactions or redox titrations.

4. In the study suggesting that the two phases of A_1^- reoxidation are due to the participation of two phylloquinones (Q_K-A and Q_K-B), the absence of an effect of the membrane potential on the relative amplitudes of the two phases was taken as evidence that electron transfer from each of the two phylloquinones to F_X is much faster than the reverse reaction [29], i.e., $P700^+Q_K-A^-$ and $P700^+Q_K-B^-$ are well above $P700^+F_X^-$ in free energy. It appears to us, that the amplitude ratio of the two phases in the two-branch model should depend on the yields of primary charge separation in the two branches and is unlikely to be affected by the membrane potential, whatever the reaction free energy ΔG^0 for electron transfer from the phylloquinones to F_X . Hence, accepting the two-branch model, the observation cited above cannot be used to estimate ΔG^0 .

Despite these uncertainties about the reduction potential of A_1 , there is no doubt that it must be well below that of the terminal acceptor complex F_A/F_B ($E_m \approx -530$ mV versus NHE), and is most likely close to or below that of F_X ($E_m \approx -700$ mV). To explain such a low potential of phylloquinone, it was suggested that the environment of A_1 is aprotic and may provide electron repulsive groups [10,58]. Refer-

ring to data by Prince and coworkers [51], two papers [27,60] assumed that the half-reduction potential of phylloquinone (being the same as that of menaquinone) in the aprotic solvent dimethylformamide (DMF) is -465 mV versus NHE; the much lower potential of phylloquinone in the A_1 site was attributed to an extremely low acceptor property of the A_1 site. It appears to us that the cited potential of phylloquinone and menaquinone in DMF is not consistent with the original data [51], where the potentials were measured versus a standard calomel electrode (SCE); listed potentials for menaquinones range from -746 mV (menaquinone-0) to -705 mV (menaquinone-7) [51]. Apparently, the value of -465 mV versus NHE in [27,60] was obtained by adding 244 mV to the potential versus SCE measured in DMF. This conversion would be valid in aqueous solution, but may fail in aprotic solvents because of the junction potential between the aqueous reference electrode and the bulk solution [53]. Instead, one may use the half-reduction potential of ferrocene as a reference that was measured to be $+524$ mV versus SCE under the conditions of the quinone measurements [51]. The formal potential of ferrocene is assumed to be independent of the solvent [33], and was reported to be $+400$ or $+425$ mV versus NHE in water [33,71]). In a first approximation, one may therefore assume that potentials referred to NHE are about 100 mV lower than those versus SCE measured in [51]. This approach would yield potentials of about -850 to -800 mV versus NHE for different menaquinones in DMF, well low enough for what is required for phylloquinone in the A_1 site.

The 2.5-\AA structure of the PS I complex from *S. elongatus* should allow to analyse the differences in the quinone environments that might explain the strikingly different reduction potentials of menaquinone-9 in the Q_A site of the reaction centre from *Rp. viridis* ($E_m \approx -150$ mV [52]) and phylloquinone in the A_1 site of PS I ($E_m \leq -700$ mV). We would like to mention a few points that may be relevant in this respect:

- Amongst the main factors governing the redox potential of cofactors in situ are differential solvation interactions of the oxidised and reduced form with the protein environment. A favourable interaction of the protein with the negatively charged, reduced

species can strongly increase the redox potential. In the case of the reaction centre of *Rp. viridis*, Q_A is situated in a highly polar environment with many polar groups and internal water molecules. Interaction with these groups will decrease the desolvation penalty for the (negatively) charged quinone and hence increase its reduction potential [36]. In PS I, a highly nonpolar environment could preserve the low reduction potential of A_1 . It is worth mentioning in this context that, in contrast to the quinone acceptor complex of the purple bacterial reaction centres, no proton transfer has to be coupled to electron transfer in PS I.

- The positive charge on the non-heme iron on the acceptor side of the purple bacterial reaction centre raises the potential in the quinone region [36] and may contribute to the higher reduction potential of Q_A compared to A_1 . Similarly, the presence of two negative charges on F_X (including the cysteine ligands) may decrease the potential of A_1 .
- For both phylloquinones in PS I, only one of the carbonyls accepts a hydrogen bond (from a backbone NH group of a leucine residue) [17,30]. In *Rp. viridis*, there is an additional hydrogen bond, from a histidine residue to the second carbonyl of Q_A , that should stabilise the semiquinone anion state and hence increase the reduction potential of Q_A compared to that of A_1 in PS I.
- As pointed out by Iwaki and Itoh [26], π - π interactions between a quinone ring and an aromatic residue should destabilise the reduced form of the quinone. Such an effect is probably exerted by TrpA679 and TrpB677 situated at plane-to-plane distances of 3.0–3.5 Å from the phylloquinones in PS I [17,30]. In *Rp. viridis*, π - π stacking between Q_A and TrpM250 is much weaker (plane-to-plane distance, 4.7 Å [47]).

3.3. How do reported electron transfer rates compare with the cofactor distances?

The relation between electron transfer rates and distances between the cofactors in PS I has been discussed previously ([7,32] and references therein) on the basis of the 4.5-Å and the 4-Å structure of PS I. Most of these discussions used a simple semi-empirical relation for the rate k_{et} (in s^{-1}) of intra-

protein electron transfer proposed by Moser and Dutton [48]:

$$\log k_{et} = 15 - 0.6R - 3.1(\Delta G^0 + \lambda)^2 / \lambda \quad (2)$$

where R is the shortest edge-to-edge distance (in Å) between donor and acceptor, ΔG^0 the standard reaction free energy (in eV), and λ the reorganisation energy (in eV). The ‘optimal’ (maximal) rate for a given distance is obtained for the special case $-\Delta G^0 = \lambda$. Except for primary charge separation (see (1) below) and charge recombination in the pair $P700^+A_1^-$ (see (2) below), no obvious violation of Eq. 2 has been reported. A more refined analysis will be possible on the basis of the 2.5 Å structure of PS I [17,30]. At the present stage (the co-ordinates of the 2.5 Å structure were not yet released when we finished this manuscript), we restrict ourselves to a few comments:

1. Primary charge separation (electron transfer from excited P700 to A_0 over an edge-to-edge distance of about 13 Å (according to the 4-Å structure [32])) is much faster (k_{et} in the order of $10^{12} s^{-1}$; see Section 3.1) than the optimal rate of about $10^7 s^{-1}$ calculated from Eq. 2 for $-\Delta G^0 = \lambda$. As pointed out previously [7,32], this discrepancy strongly suggests that an ‘accessory’ chlorophyll eC-B₂ and/or eC-A₂ is involved in this electron transfer.
2. The rate of charge recombination in the pair $P700^+A_1^-$ (presumably about $4 \times 10^3 s^{-1}$ in intact PS I [7] and up to $10^5 s^{-1}$ in PS I devoid of F_X , F_A , and F_B [9]) exceeds the optimal rate of $5 \times 10^2 s^{-1}$ calculated from Eq. 2 with $-\Delta G^0 = \lambda$ and $R = 20.5 \text{ Å}$ [32]. One may consider two possibilities: (a) The electronic coupling between A_1^- and $P700^+$ is enhanced by the chlorophylls located in between (see Fig. 1), including the possibility of some charge delocalisation between A_1^- and A_0 or between $P700^+$ and an ‘accessory’ chlorophyll eC-B₂ and/or eC-A₂. (b) The protein structure between $P700$ and A_1 provides particularly favourable electron transfer pathways (see [3] for an approach to establish and to treat such pathways).
3. According to the 2.5-Å structure [17,30], the distance between the centre of F_X and the midpoint of the two oxygen atoms of phylloquinone Q_K-A and of phylloquinone Q_K-B are 14.2 and 14.1 Å,

respectively. The benzyl rings of both phylloquinones are oriented towards F_X , thus minimising the edge-to-edge distances to F_X , as suggested previously from an electron transfer study [57]. Taking into account also the orientation of F_X , the shortest edge-to-edge distance to the phylloquinones should be in the order of 8 Å for both branches (for F_X , we considered the sulphur atoms of the cysteine ligands as edge atoms, because they receive a considerable electron density upon reduction of [4Fe–4S] clusters [7,49]). Inserting this distance in Eq. 2, the faster phase ($k_{\text{et}} \approx 5 \times 10^7 \text{ s}^{-1}$) of A_1^- reoxidation (see Section 2.2) can be obtained with a small driving force and an unspectacular reorganisation energy (e.g., $\Delta G^0 = -0.1 \text{ eV}$ and $\lambda = 1 \text{ eV}$, or $\Delta G^0 = 0$ and $\lambda = 0.8 \text{ eV}$). If the slower phase of A_1^- reoxidation ($k_{\text{et}} \approx 4 \times 10^6 \text{ s}^{-1}$) reflects electron transfer from the other phylloquinone to F_X (see Section 3.1), the slower rate may be due to a higher reorganisation energy and/or a lower driving force, rather than to a larger distance between the cofactors.

4. Note added in proof

After submission of the manuscript, several articles appeared which are relevant to the question whether two electron transfer branches are active in PS I. Guergova-Kuras et al. [22] studied the effect of mutations of tryptophan residues supposed to be close to the phylloquinones on the *in vivo* kinetics of A_1^- reoxidation in whole cells of *C. reinhardtii*. While the mutation PsaA-W693F slowed specifically the slower phase (from $t_{1/2} \approx 150 \text{ ns}$ to $\approx 400 \text{ ns}$), the mutation PsaB-W673F slowed specifically the faster phase (from $t_{1/2} \approx 13 \text{ ns}$ to $\approx 70 \text{ ns}$). The double mutation PsaA-W693F/PsaB-W673F resulted in a slowdown of both phases. As pointed out in [22], these effects could be by far most easily explained with the assumption that the faster phase of A_1^- reoxidation reflects electron transfer in the PsaB-branch, and the slower one in the PsaA-branch, and that mutation of either tryptophan slows down reoxidation of the close by phylloquinone.

Hastings and Sivakumar [23] reported a Fourier transform infrared absorption spectrum associated

with photoaccumulation of A_1^- in samples from *Synecocystis* sp. PCC 6803 devoid of Fe–S centres F_A , F_B , and F_X . The complexity of the spectra in various spectral regions was taken as indication that two structurally distinct phylloquinones were photoaccumulated, which could correspond to the phylloquinones on the PsaA and PsaB branches.

Purton and coworkers [54] investigated the environment of the phylloquinone acceptors by site-directed mutagenesis of two tryptophan residues (W693 and W702) in the PsaA subunit of PS I from *C. reinhardtii*. Replacement of W693 with either histidine or leucine altered the electronic structure of the photoaccumulated A_1^- radical and slowed forward electron transfer (by a factor of ~ 3) as measured by the decay of the electron spin-polarised signal from the radical pair $P700^+A_1^-$ at 260 K (the same mutations of W702 had no effect). The authors pointed out that the limited time resolution of this technique only allows to detect the slow phase of A_1^- reoxidation, which, in agreement with the results of Guergova-Kuras et al. [22], is proposed to occur in the PsaA-branch.

Acknowledgements

We thank Drs Norbert Krauss and Jean-Marc Moulis for communicating data prior to publication, and Roger Prince and Peter Wardman for discussions on reduction potentials of quinones.

References

- [1] D. Béal, F. Rappaport, P. Joliot, *Rev. Sci. Instrum.* 70 (1999) 202–207.
- [2] G.S. Beddard, *Phil. Trans. R. Soc. Lond. A* 356 (1998) 421–448.
- [3] D.N. Beratan, J.N. Betts, J.N. Onuchic, *Science* 252 (1991) 1285–1288.
- [4] J. Biggins, P. Mathis, *Biochemistry* 27 (1988) 1494–1500.
- [5] C.H. Bock, A.J. Van der Est, K. Brettel, D. Stehlik, *FEBS Lett.* 247 (1989) 91–96.
- [6] K. Brettel, *FEBS Lett.* 239 (1988) 93–98.
- [7] K. Brettel, *Biochim. Biophys. Acta* 1318 (1997) 322–373.
- [8] K. Brettel, in: G. Garab (Ed.), *Photosynthesis: Mechanisms and Effects*, Vol. 1, Kluwer Academic Publishers, Dordrecht, 1998, pp. 611–614.

- [9] K. Brettel, J.H. Golbeck, *Photosynth. Res.* 45 (1995) 183–193.
- [10] K. Brettel, P. Sétif, P. Mathis, *FEBS Lett.* 203 (1986) 220–224.
- [11] K. Brettel, M.H. Vos, *FEBS Lett.* 447 (1999) 315–317.
- [12] M. Byrdin, I. Rimke, E. Schlodder, D. Stehlik, T.A. Roelofs, *Biophys. J.* 79 (2000) 992–1007.
- [13] J. Deisenhofer, O. Epp, R. Huber, H. Michel, *J. Mol. Biol.* 180 (1984) 385–398.
- [14] A. Diaz-Quintana, W. Leibl, H. Bottin, P. Sétif, *Biochemistry* 37 (1998) 3429–3439.
- [15] M.C.W. Evans, S. Purton, P. Vaishali, D. Wright, P. Heathcote, S.E.J. Rigby, *Photosynth. Res.* 61 (1999) 33–42.
- [16] N. Fischer, P. Sétif, J.-D. Rochaix, *J. Biol. Chem.* 274 (1999) 23333–23340.
- [17] P. Fromme, P. Jordan, N. Krauss, *Biochim. Biophys. Acta* 1507 (2001) 5–31.
- [18] B. Gobets, J.P. Dekker, R. van Grondelle, in: G. Garab (Ed.), *Photosynthesis: Mechanisms and Effects*, Vol. 1, Kluwer Academic Publishers, Dordrecht, 1998, pp. 503–508.
- [19] B. Gobets, R. van Grondelle, *Biochim. Biophys. Acta* 1507 (2001) 80–99.
- [20] J.H. Golbeck, *Photosynth. Res.* 61 (1999) 107–144.
- [21] J.H. Golbeck, D.A. Bryant, in: C.P. Lee (Ed.), *Current Topics in Bioenergetics*, Vol. 16, Academic Press, San Diego, CA, 1991, pp. 83–177.
- [22] M. Guergova-Kuras, B. Boudreaux, A. Joliot, P. Joliot, K. Redding, *Proc. Natl. Acad. Sci. USA* 98 (2001) 4437–4442.
- [23] G. Hastings, V. Sivakumar, *Biochemistry* 40 (2001) 3681–3689.
- [24] P. Heathcote, J.A. Hanley, M.C.W. Evans, *Biochim. Biophys. Acta* 1144 (1993) 54–61.
- [25] B. Hecks, J. Breton, W. Leibl, K. Wulf, H.-W. Trissl, *Biochemistry* 33 (1994) 8619–8624.
- [26] M. Iwaki, S. Itoh, *Biochemistry* 30 (1991) 5347–5352.
- [27] M. Iwaki, S. Itoh, *Plant Cell Physiol.* 35 (1994) 983–993.
- [28] T.W. Johnson, G. Shen, B. Zybailov, D. Kolling, R. Reategui, S. Beauparlant, I.R. Vassiliev, D.A. Bryant, A.D. Jones, J.H. Golbeck, *J. Biol. Chem.* 275 (2000) 8523–8530.
- [29] P. Joliot, A. Joliot, *Biochemistry* 38 (1999) 11130–11136.
- [30] P. Jordan, P. Fromme, O. Klukas, H.T. Witt, W. Saenger, N. Krauss, *Nature* 411 (2001) 909–917.
- [31] R. Jordan, U. Nissau, E. Schlodder, in: G. Garab (Ed.), *Photosynthesis: Mechanisms and Effects*, Vol. 1, Kluwer Academic Publishers, Dordrecht, 1998, pp. 663–666.
- [32] O. Klukas, W.-D. Schubert, P. Jordan, N. Kraus, P. Fromme, H.T. Witt, W. Saenger, *J. Biol. Chem.* 274 (1999) 7361–7367.
- [33] H.-M. Koepp, H. Wendt, H. Strehlow, *Z. Elektrochem.* 64 (1960) 483–491.
- [34] R. Kümmerle, J. Gaillard, P. Kyritsis, J.-M. Moulis, *J. Biol. Inorg. Chem.* 6 (2001) 446–451.
- [35] K.V. Lakshmi, Y.-S. Jung, J.H. Golbeck, G.W. Brudvig, *Biochemistry* 38 (1999) 13210–13215.
- [36] C.R. Lancaster, H. Michel, B. Honig, M.R. Gunner, *Biophys. J.* 70 (1996) 2469–2492.
- [37] W. Leibl, B. Toupance, J. Breton, *Biochemistry* 34 (1995) 10237–10244.
- [38] C. Lelong, E.J. Boekema, J. Kruip, H. Bottin, M. Rögner, P. Sétif, *EMBO J.* 15 (1996) 2160–2168.
- [39] J. Lüneberg, P. Fromme, P. Jekow, E. Schlodder, *FEBS Lett.* 338 (1994) 197–202.
- [40] F. MacMillan, J. Hanley, L. van der Weerd, M. Knüpling, S. Un, A.W. Rutherford, *Biochemistry* 36 (1997) 9297–9303.
- [41] R. Malkin, *FEBS Lett.* 208 (1986) 343–346.
- [42] A.A. Mamadova, M.D. Mamedov, K.N. Gourovskaya, I.R. Vassiliev, J.H. Golbeck, A.Y. Semenov, *FEBS Lett.* 462 (1999) 421–424.
- [43] R.A. Marcus, *J. Chem. Phys.* 24 (1956) 966–978.
- [44] R.A. Marcus, N. Sutin, *Biochim. Biophys. Acta* 811 (1985) 265–322.
- [45] P. Mathis, P. Sétif, *FEBS Lett.* 237 (1988) 65–68.
- [46] D. Mi, S. Lin, R.E. Blankenship, *Biochemistry* 38 (1999) 15231–15237.
- [47] H. Michel, O. Epp, J. Deisenhofer, *EMBO J.* 5 (1986) 2445–2451.
- [48] C.C. Moser, P.L. Dutton, *Biochim. Biophys. Acta* 1101 (1992) 171–176.
- [49] L. Noodleman, D.A. Case, in: R. Cammack (Ed.), *Advances in Inorganic Chemistry*, Vol. 38, Iron–Sulfur Proteins, Academic Press, San Diego, CA, 1992, pp. 423–470.
- [50] M. Polm, K. Brettel, *Biophys. J.* 74 (1998) 3173–3181.
- [51] R.C. Prince, P.L. Dutton, J.M. Bruce, *FEBS Lett.* 160 (1983) 273–276.
- [52] R.C. Prince, J.S. Leigh, P.L. Dutton, *Biochim. Biophys. Acta* 440 (1976) 622–636.
- [53] R.C. Prince, P. Lloyd-Williams, J.M. Bruce, P.L. Dutton, *Methods Enzymol.* 125 (1986) 109–119.
- [54] S. Purton, D.R. Stevens, I.P. Muhiuddin, M.C.W. Evans, S. Carter, S.E.J. Rigby, P. Heathcote, *Biochemistry* 40 (2001) 2167–2175.
- [55] H. Rupp, A. de la Torre, D.O. Hall, *Biochim. Biophys. Acta* 548 (1979) 552–564.
- [56] S. Savikhin, X. Wu, P.R. Chitnis, W.S. Struve, *Biophys. J.* 79 (2000) 1573–1586.
- [57] E. Schlodder, K. Falkenberg, M. Gergeleit, K. Brettel, *Biochemistry* 37 (1998) 9466–9476.
- [58] H.-U. Schoeder, W. Lockau, *FEBS Lett.* 199 (1986) 23–27.
- [59] T. Schwartz, K. Brettel, in: P. Mathis (Ed.), *Photosynthesis: From Light to Biosphere*, Vol. 2, Kluwer Academic Publishers, Dordrecht, 1995, pp. 43–46.
- [60] A.Y. Semenov, I.R. Vassiliev, A. van der Est, M.D. Mamedov, B. Zybailov, G. Shen, D. Stehlik, B. Diner, P.R. Chitnis, J.H. Golbeck, *J. Biol. Chem.* 275 (2000) 23429–23438.
- [61] P. Sétif, H. Bottin, *Biochemistry* 33 (1994) 8495–8504.
- [62] P.Q.Y. Sétif, H. Bottin, *Biochemistry* 34 (1995) 9059–9070.
- [63] P. Sétif, K. Brettel, *Biochemistry* 32 (1993) 7846–7854.
- [64] V.P. Shinkarev, I.R. Vassiliev, J.H. Golbeck, *Biophys. J.* 78 (2000) 363–372.
- [65] K. Sigfridsson, Ö. Hansson, P. Brzezinski, *Proc. Natl. Acad. Sci. USA* 92 (1995) 3458–3462.
- [66] H.-W. Trissl, K. Wulf, *Biospectroscopy* 1 (1995) 71–82.

- [67] A. van der Est, C. Bock, J. Golbeck, K. Brettel, P. Sétif, D. Stehlik, *Biochemistry* 33 (1994) 11789–11797.
- [68] A. van der Est, *Biochim. Biophys. Acta* 1507 (2001) 212–225.
- [69] I.R. Vassiliev, Y.-S. Jung, F. Yang, J.H. Golbeck, *Biophys. J.* 74 (1998) 2029–2035.
- [70] F. Yang, G. Shen, W.M. Schluchter, B.L. Zybailov, A.O. Ganago, I.R. Vassiliev, D.A. Bryant, J.H. Golbeck, *J. Phys. Chem. B* 102 (1998) 8288–8299.
- [71] P. Yeh, T. Kuwana, *J. Electrochem. Soc.* 123 (1976) 1334–1339.
- [72] B. Zybailov, A. van der Est, S.G. Zech, C. Teutloff, T.W. Johnson, G. Shen, R. Bittl, D. Stehlik, P.R. Chitnis, J.H. Golbeck, *J. Biol. Chem.* 275 (2000) 8531–8539.